Modeling and Thermal Analysis of a Ground Cooling System for Drilling Fluids in Ultra-Deep Wells

Jiangshuai Wang[1,*], Zixiao Song[1], Yufei Chen[2], Bohan Zheng[1], Song Deng[1], Ke Xu[1], Bei Wang[1] and Qianyu Ren[1]

[1] School of Petroleum and Natural Gas Engineering, Changzhou University, Changzhou, 213164, China

[2] CNPC Engineering Technology R&D Company Limited, Beijing, 100085, China

INFORMATION

Keywords:
Ultra-deep wells
cooling system model
cooling law
drilling fluid temperature control
wellbore temperature environment

DOI: 10.23967/j.rimni.2025.10.68949

SCIPEDIA Revista Internacional de Métodos Numéricos para Cálculo y Diseño en Ingeniería

Revista Internacional Métodos numéricos para cálculo y diseño en ingeniería RIMNI

In cooperation with CIMNE

Modeling and Thermal Analysis of a Ground Cooling System for Drilling Fluids in Ultra-Deep Wells

Jiangshuai Wang[1,*], Zixiao Song[1], Yufei Chen[2], Bohan Zheng[1], Song Deng[1], Ke Xu[1], Bei Wang[1] and Qianyu Ren[1]

[1]School of Petroleum and Natural Gas Engineering, Changzhou University, Changzhou, 213164, China

[2]CNPC Engineering Technology R&D Company Limited, Beijing, 100085, China

ABSTRACT

Elevated downhole temperatures in ultra-deep wells (>8000 m) accelerate thermal degradation of drilling fluids and tools, reducing operational safety and efficiency. The reduction of wellbore temperature is an important issue. In this paper, a cooling system model for a drilling fluid was designed. Additionally, a comprehensive analysis of the heat transfer behavior within ultra-deep wells was conducted. A miniaturized heat exchange cooling device was used to simulate various conditions, including fluid media, flow rate, drilling fluid/coolant temperature, and heat exchanger structure. This analysis elucidates the impact of various factors on cooling efficiency. The experimental results show that the cooling effect is best at a medium flow rate, with a refrigerant temperature of −10°C reducing the temperature of pure water from 60°C to 32°C. The experiment also found that the higher the temperature of the pure water and the lower the temperature of the coolant, the better the heat transfer efficiency. For water-based drilling fluid, the optimum cooling flow rate is around 0.52 m/s, with an average Reynolds number of 4966, and the maximum cooling range can exceed 30°C. Furthermore, the coil heat exchanger significantly improves the cooling rate compared to the straight-tube heat exchanger, although the pressure difference also increases. The cooling rate of oil-based drilling fluid at high flow rates is greater than that of water-based drilling fluid, and the pressure difference in the coil heat exchanger for oil-based drilling fluid, which has higher viscosity, increases significantly. This research provides an experimental basis for the design and optimization of drilling fluid surface cooling systems, which is crucial for improving the safety and efficiency of deep and ultra-deep wells drilling.

OPEN ACCESS

Received: 10/06/2025

Accepted: 15/08/2025

Published: 27/11/2025

DOI
10.23967/j.rimni.2025.10.68949

Keywords:
Ultra-deep wells
cooling system model
cooling law
drilling fluid temperature control
wellbore temperature environment

1 Introduction

In modern oil and gas drilling operations, drilling fluid is a key working medium, which has many functions such as lubrication, debris removal, wellbore stability, and formation pressure control. The

*Correspondence: Jiangshuai Wang (wjs125126@163.com).

performance of drilling fluid directly affects the drilling efficiency and safety, and its management and optimization are the key links of drilling engineering [1–3]. With the increasing demand for global energy, drilling operations are expanding to deeper and more complex geological structures. However, with the increase of drilling depth and formation temperature, the temperature of drilling fluid tends to increase significantly, which affects the physical and chemical properties of the drilling fluid, and may reduce drilling efficiency and increase safety hazards [4–6]. Under high temperature conditions, the viscosity of drilling fluid increases and the fluidity decreases, which may even lead to the failure of the drilling fluid and pose a threat to the overall operation [7–9].

Drilling fluid temperature control: a serious challenge drilling fluid temperature control has become an urgent technical problem to be solved in deep and ultra-deep well drilling [10–13]. High temperature will accelerate the degradation of chemical treatment agents in drilling fluid, reduce their stability, increase equipment wear, and even lead to serious accidents such as wellbore collapse. Therefore, effective temperature control of drilling fluid is very important to prolong its service life, improve drilling efficiency and ensure the safety of operators.

Existing research and its limitations. Previous studies have explored a variety of methods to control drilling fluid temperature, Ref. [14] included the use of high-performance drilling fluid [15–19] and advanced cooling technology [20–24]. However, these studies usually focus on specific aspects of temperature control, such as the performance of drilling fluids at high temperatures or the efficiency of cooling systems. Few studies have comprehensively solved the design and optimization of drilling fluid ground cooling systems, especially in the context of deep and ultra-deep wells. In addition, the existing research often lacks detailed experimental verification of the cooling law under various conditions, which is crucial for practical applications.

The innovation of current research in order to solve these gaps, the current research investigated the feasibility of ground cooling drilling fluid, and tested its cooling effect under various conditions through laboratory experiments. Using a small heat exchanger cooling device, we simulated different fluid media, flow rates, drilling fluid coolant temperatures, and heat exchanger structures. This method provides a comprehensive understanding of the factors affecting the cooling effect of the ground cooling system. The purpose of this study is to provide a scientific basis for the design and optimization of the drilling fluid surface cooling system, which is crucial to improving the safety and efficiency of deep and ultra-deep well drilling.

When analyzing the influence of the temperature difference between the high temperature fluid and the low temperature coolant on the heat transfer efficiency, we can use the Fourier law, which points out that the heat flux is proportional to the temperature gradient [25]. This means that the greater the temperature difference, the greater the heat flux density, and the higher the heat transfer efficiency. The experimental results also confirm this point. When the temperature of high temperature fluid (such as pure water) is much higher than that of low temperature coolant, the heat transfer efficiency is significantly improved. Therefore, in the design of the drilling fluid ground cooling system, it is very important to reasonably select the temperature of high temperature fluid and low temperature coolant to make full use of the effect of temperature difference on heat transfer efficiency.

Building upon existing surface cooling technologies, this study proposes an optimized structural configuration specifically designed for ultra-deep well applications (>8000 m). The proposed system has undergone comprehensive laboratory validation, demonstrating its effectiveness in downhole temperature reduction under controlled conditions. The system cools the returned drilling fluid and then injects it into the drill pipe for circulating drilling, thereby improving the wellbore temperature environment. The system reduces downhole temperatures by 30°C–44°C, mitigating risks of fluid

thermal degradation and tool failure, and ensures the safe and efficient drilling of deep wells, ultra-deep wells and shale oil and gas horizontal wells.

In summary, the straight-tube heat exchanger proposed by Zhang et al. fails to account for the extreme thermal conditions encountered in ultra-deep well drilling. Meanwhile, the ground-source cooling system investigated by Arghand et al. exhibits prohibitively high energy consumption. Additionally, the helical groove tube design introduced by Deng et al. was validated solely for water-based drilling fluids, leaving oil-based systems unexamined. This study seeks to address these critical research gaps by conducting a comprehensive experimental investigation of a drilling fluid ground cooling system. The findings will contribute to the development of optimized cooling solutions, enhancing thermal management efficiency in deep and ultra-deep well drilling operations.

2 Design of Drilling Fluid Ground Cooling Device

2.1 Overall Design of the Device

This section introduces the drilling fluid ground cooling system used in the experiment in detail. As shown in Fig. 1, it is the flowchart of the experimental setup. This system aims to simulate the cooling effect in the actual drilling process through precise control of the experimental conditions and study the influence of different parameters on the cooling efficiency. As shown in Figs. 2 and 3, the experimental setup is composed of several key modules, including the low-temperature coolant module, the heat exchanger module, the high-temperature drilling fluid module, and the computer data acquisition module. Each module is equipped with the necessary high-precision instruments, such as thermometers, pressure gauges and flow meters, to ensure the accuracy of the experimental data. The heat exchanger module is specially designed with two structural options-split straight tube and custom coil to compare and analyze the influence of different heat exchanger structures on the cooling effect. The inner diameter of the heat exchange outer cylinder is set according to the space required for the temperature sensor layout, the appearance diameter of the coil, the heat exchange efficiency, and the hot fluid supply capacity. The material is stainless steel, and the existing experimental device is 265 mm. Through this device, we can simulate and study the cooling performance of a variety of fluid media under different flow rates and temperature conditions, and provide a scientific basis for the design and optimization of the ground cooling system.

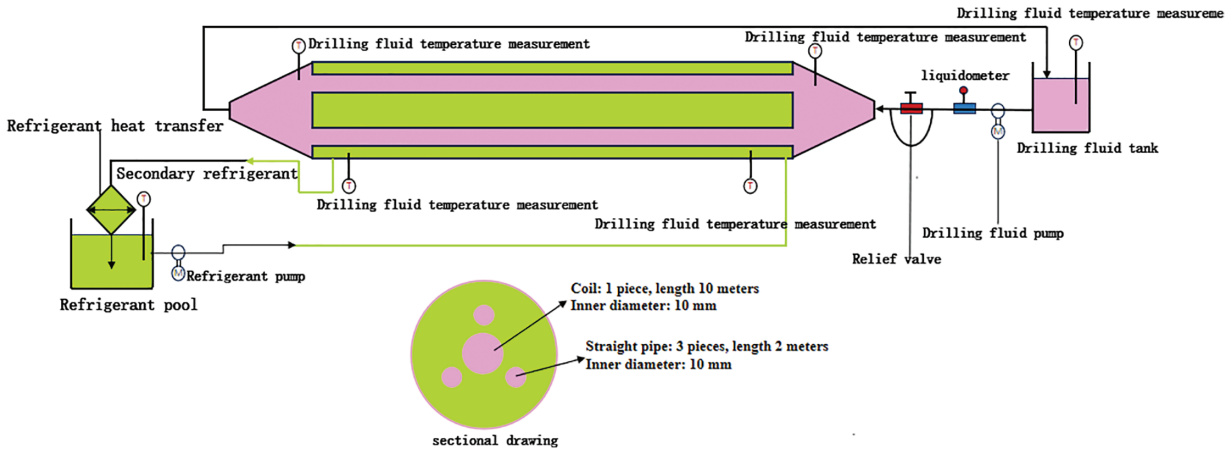

Figure 1: Miniaturized drilling fluid heat exchange cooling device schematic diagram

(a) (b) (c)

Figure 2: The core module of the device: (**a**) Refrigeration module; (**b**) Shunt straight pipe; (**c**) Custom coil

Figure 3: Miniaturized drilling fluid heat exchange cooling device physical diagram

2.2 Experimental Steps Description

After the installation and debugging of the experimental equipment are completed, the experiment is carried out according to the following main steps:

1) First, the liquid to be tested (water-based drilling fluid, oil-based drilling fluid, etc.) is placed on the right side of the drilling fluid heating reservoir and heated to a predetermined temperature. Then, the low-temperature water bath is turned on, and the temperature of the coolant (generally water + ethylene glycol) is set to a predetermined temperature.

2) Open the constant current pump and pump the liquid to be tested into the middle heat exchanger at a predetermined speed, monitor and record the temperature of the liquid to be tested at the inlet and outlet of the heat exchanger, as well as the coolant inlet and outlet temperatures.

3) Install the safety relief valve and the U-shaped buffer pipe at the inlet end to improve the equipment's safety. Use the pressure gauge to measure the inlet pressure (P1). The pressure value mainly serves to monitor the flow state of the fluid in the pipeline and the pressure loss required by the cooling system under different conditions.

4) The frequency converter is used to control the speed of the motor in order to adjust the flow rate of the liquid to be measured and conduct the cooling experiment under different flow rates. In addition, the temperatures of the test liquid and the coolant, the composition of the test liquid, and the structure of the heat exchanger can also be adjusted to simulate cooling experiments under different conditions.

5) After the experiment is finished, the pipeline is cleaned, the power supply is turned off, and the experimental data are processed.

2.3 Setting of Experimental Conditions

In order to complete the indoor simulation experiment of ground cooling and cooling under different fluid media, flow rates, drilling fluid/coolant temperatures, heat exchanger structures, and other conditions, 66 groups of experiments were set up, taking into account the working ability of the device. The specific conditions are shown in Table 1. It should be noted that there will be deviations in the experimental process under the following conditions.

Table 1: Number of experimental groups and experimental conditions

Serial number	Fluid medium	Flow velocity (m/s)	Flow temperature (°C)	Refrigerant temperature (°C)	Heat exchanger structure
1	Water	0.1	60	−10	Straight tube
2	Water	0.1	60	−5	Straight tube
3	Water	0.1	60	0	Straight tube
4	Water	0.1	60	5	Straight tube
5	Water	0.1	60	10	Straight tube
6	Water	0.2	60	−10	Straight tube
7	Water	0.2	60	−5	Straight tube
8	Water	0.2	60	0	Straight tube
9	Water	0.2	60	5	Straight tube
10	Water	0.2	60	10	Straight tube
11	Water	0.3	60	−10	Straight tube
12	Water	0.3	60	−5	Straight tube
13	Water	0.3	60	0	Straight tube
14	Water	0.3	60	5	Straight tube
15	Water	0.3	60	10	Straight tube
16	Water	0.4	60	−10	Straight tube
17	Water	0.4	60	−5	Straight tube
18	Water	0.4	60	0	Straight tube
19	Water	0.4	60	5	Straight tube
20	Water	0.4	60	10	Straight tube
21	Water	0.5	60	−10	Straight tube
22	Water	0.5	60	−5	Straight tube
23	Water	0.5	60	0	Straight tube
24	Water	0.5	60	5	Straight tube
25	Water	0.5	60	10	Straight tube

(Continued)

Table 1 (continued)

Serial number	Fluid medium	Flow velocity (m/s)	Flow temperature (°C)	Refrigerant temperature (°C)	Heat exchanger structure
26	Water	0.5	40	−10	Straight tube
27	Water	0.5	50	−10	Straight tube
28	Water	0.5	60	−10	Straight tube
29	Water	0.5	70	−10	Straight tube
30	Water	0.5	80	−10	Straight tube
31	Water + Bentonite	0.1	60	−10	Straight tube
32	Water + Bentonite	0.2	60	−5	Straight tube
33	Water + Bentonite	0.3	60	0	Straight tube
34	Water + Bentonite	0.4	60	5	Straight tube
35	Water + Bentonite	0.5	60	10	Straight tube
36	Water + Bentonite	0.3	40	0	Straight tube
37	Water + Bentonite	0.3	50	0	Straight tube
38	Water + Bentonite	0.3	70	0	Straight tube
39	Water + Bentonite	0.3	80	0	Straight tube
40	Water + Bentonite	0.3	60	−10	Straight tube
41	Water + Bentonite	0.3	60	−5	Straight tube
42	Water + Bentonite	0.3	60	5	Straight tube
43	Water + Bentonite	0.3	60	10	Straight tube
44	Water + Bentonite	0.1	60	0	Coil
45	Water + Bentonite	0.2	60	0	Coil
46	Water + Bentonite	0.3	60	0	Coil
47	Water + Bentonite	0.4	60	0	Coil
48	Water + Bentonite	0.5	60	0	Coil
49	Oil + Bentonite	0.1	60	0	Straight tube
50	Oil + Bentonite	0.2	60	0	Straight tube
51	Oil + Bentonite	0.3	60	0	Straight tube
52	Oil + Bentonite	0.4	60	0	Straight tube
53	Oil + Bentonite	0.5	60	0	Straight tube
54	Oil + Bentonite	0.3	40	0	Straight tube
55	Oil + Bentonite	0.3	50	0	Straight tube
56	Oil + Bentonite	0.3	70	0	Straight tube
57	Oil + Bentonite	0.3	80	0	Straight tube
58	Oil + Bentonite	0.3	60	−10	Straight tube
59	Oil + Bentonite	0.3	60	−5	Straight tube
60	Oil + Bentonite	0.3	60	5	Straight tube
61	Oil + Bentonite	0.3	60	10	Straight tube
62	Oil + Bentonite	0.1	60	0	Coil
63	Oil + Bentonite	0.2	60	0	Coil
64	Oil + Bentonite	0.3	60	0	Coil

(Continued)

Table 1 (continued)

Serial number	Fluid medium	Flow velocity (m/s)	Flow temperature (°C)	Refrigerant temperature (°C)	Heat exchanger structure
65	Oil + Bentonite	0.4	60	0	Coil
66	Oil + Bentonite	0.5	60	0	Coil

3 Experimental Analysis

3.1 Experimental Analysis of the Influence of Different Factors on Pure Water and Straight Pipe Conditions

3.1.1 Cooling Experiment Analysis under Different Flow Rate Conditions

In order to clarify the influence of flow velocity on the cooling effect, the ground cooling simulation test under different flow conditions (0.1 to 0.5 m/s) was carried out. Temperature measurements were conducted using PT100 sensors with an accuracy of ±0.5°C, while flow rate measurements were obtained using flow meters with an error range of ±2% of the full scale (FS). Each experimental condition was repeated three times, yielding a standard deviation of ±1.8°C in the cooling range. Pressure difference measurements were subject to an uncertainty of ±0.5 kPa due to the resolution limit of the U-tube manometer. The combined uncertainty was calculated through error propagation analysis, resulting in a total cooling efficiency confidence interval of ±3.5% (at a 95% confidence level). As shown in Fig. 4, 25 sets of experimental results show that the cooling effect is optimal at medium flow rates. Among them, the refrigerant at −10°C can reduce the pure water at 60°C to 32°C. Lower flow rates reduce the heat transfer coefficient due to laminar dominance, whereas excessive velocities limit contact time, as quantified by the dimensionless Fourier number. At medium flow rates, both the heat transfer coefficient and heat transfer duration are favorable.

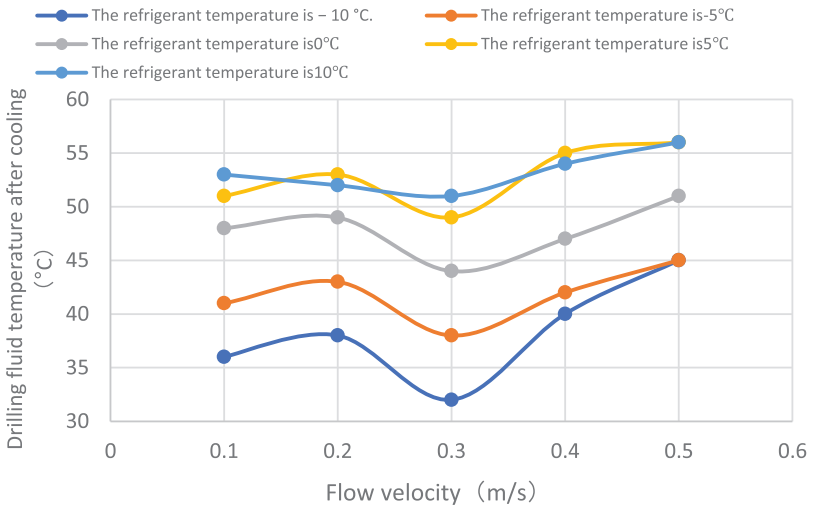

Figure 4: Comparison of cooling effect of pure water at different flow rates

Flow regimes (laminar/turbulent) are a core factor influencing cooling performance, quantified by the Reynolds number $Re = \rho vd/\mu$, where ρ is fluid density, v is flow velocity, d is pipe diameter, and μ is dynamic viscosity).

Low flow velocity (laminar-dominated, ($Re < 2000$)): The poor cooling effect at low velocities (e.g., 0.1 m/s) in the document arises because laminar flow causes fluid stratification, with heat transfer primarily via molecular diffusion, resulting in high convective thermal resistance (dominated by the boundary layer). For example, pure water at 0.1 m/s achieves only 60% of the cooling range under high-temperature-difference conditions, due to the thick laminar boundary layer hindering heat exchange.

Medium flow velocity (transitional turbulence, ($2000 < Re < 4000$)): Experiments show optimal cooling at medium velocities (e.g., 0.32 m/s ($Re \approx 4900$)), where flow approaches turbulence. Enhanced fluid mixing disrupts the boundary layer, significantly reducing convective resistance. Meanwhile, velocity remains moderate enough to ensure sufficient contact time between fluid and heat exchange surfaces (described by the Fourier number ($F_o = at/L^2$), where a is thermal diffusivity and t is contact time), enabling full heat transfer.

High flow velocity (Turbulent-dominated, ($Re > 4000$)): Turbulence intensity increases at high velocities, but reduced contact time (lower F_o) decreases total heat transfer. For instance, oil-based drilling fluids maintain a cooling range above 30°C at 2.5 m/s because their low specific heat capacity C_p amplifies temperature changes for a given heat transfer, partially offsetting shorter contact time.

As shown in Fig. 5, after further increasing the flow rate, we found that the heat transfer effect is optimal at a flow rate of 0.32 m/s. The maximum cooling range of drilling fluid is 34°C, and the average Reynolds number is about 4900, which indicates a turbulent flow state. This provides valuable guidance for the design optimization of large heat exchanger sizes and engineering parameters.

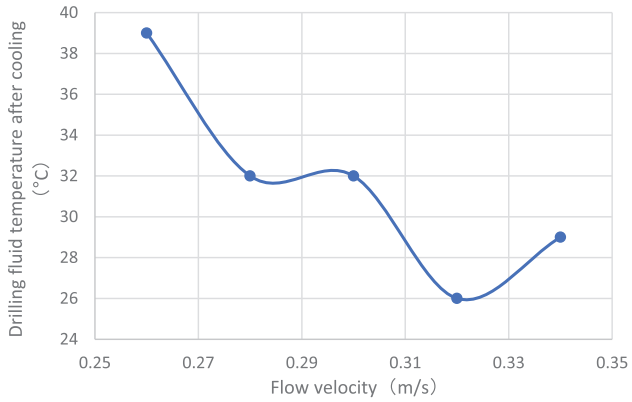

Figure 5: Comparison of cooling effect of pure water after flow rate encryption

The Nusselt number (Nu) at the optimal flow rate (0.32 m/s) was calculated as 82.4, deviating from the Dittus-Boelter prediction ($Nu = 76.1$) by 8.3%. This discrepancy suggests secondary flow effects in coiled tubes, consistent with Schmidt's curvature correction.

3.1.2 Cooling Experiment Analysis under Different Temperature Conditions

In order to clarify the influence of pure water temperature on the cooling effect, the ground cooling simulation test under different pure water temperature conditions (40°C to 80°C) was carried out. As shown in Fig. 6, the experimental results of five groups of different pure water temperature conditions

show that the higher the temperature of pure water, the larger the temperature gradient between the hot fluid and coolant, resulting in higher heat transfer efficiency. The temperature of 80°C pure water can be reduced to 45°C after passing through the indoor cooling device at a flow rate of 0.3 m/s.

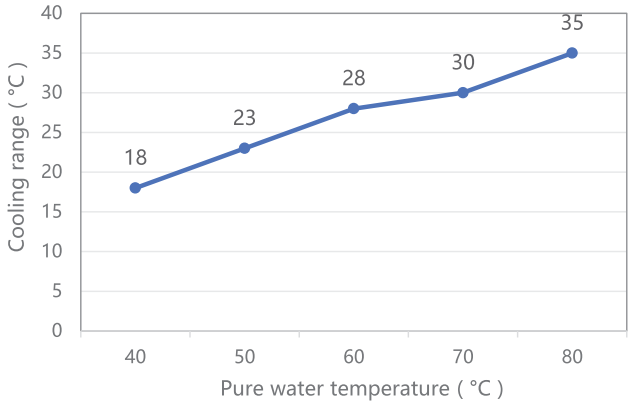

Figure 6: Comparison of cooling effect under different pure water temperatures

This is in perfect agreement with the description of Fourier's law of heat conduction. Fourier's law of heat conduction—the fundamental principle governing thermal transport—establishes that the heat flux density (q) through a material is directly proportional to the temperature gradient (∇T), with the thermal conductivity (k) as the proportionality constant. This constitutive relationship is mathematically expressed as $q = -k\nabla T$, where the negative sign denotes heat flow from high to low temperature regions.

3.1.3 Cooling Experiment Analysis under Different Refrigerant Temperature Conditions

In order to clarify the influence of the coolant temperature on the cooling effect, the ground cooling simulation test was carried out under different coolant temperature conditions (−10°C to 10°C). As shown in Fig. 7, the experimental results of five groups of different refrigerant temperatures show that the lower the temperature of the refrigerant, the greater the temperature difference between the cold and hot fluids, and the better the heat transfer effect. However, the actual temperature of the refrigerant is affected by the field working environment, and it may not be able to reach the set low temperature environment. Therefore, the influence of the working environment on the refrigeration efficiency should be considered in field applications.

Total heat transfer resistance in the cooling system is the sum of resistances across all stages ($R_{total} = R_{convection,\ hotside} + R_{conduction,\ wall} + R_{convection,\ coldside}$). Experimental observations can be explained by resistance distribution: Fourier's law $q = -k\nabla T$ indicates heat flux is proportional to temperature gradient. The temperature difference (90°C) between 80°C pure water and −10°C coolant in the document is much greater than that between 60°C pure water and 10°C coolant (50°C). The former has a higher heat flux density, and the cooling range (35°C) is significantly larger than that of the latter (9°C), confirming that "the greater the temperature difference, the stronger the driving force to overcome the total thermal resistance".

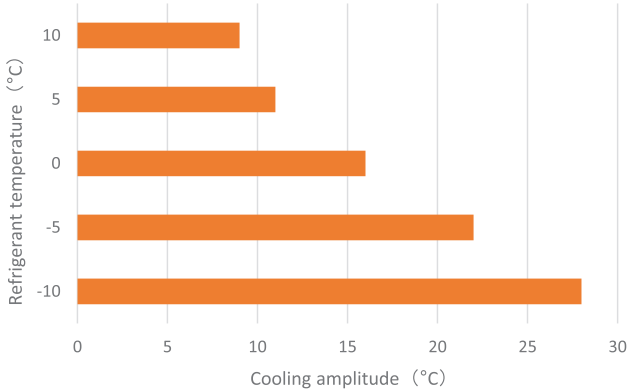

Figure 7: Comparison of cooling effects at different refrigerant temperatures

3.2 Experimental Analysis of the Influence of Different Factors on Water-Based and Straight Pipe Conditions

3.2.1 Cooling Experiment Analysis under Different Flow Rate Conditions

A water-bentonite mixture was configured to simulate water-based drilling fluid, and the ground cooling simulation test of water-based drilling fluid under different flow rates was carried out. As shown in Fig. 8, under the condition of 0.28 to 1.31 m/s, the maximum cooling range of 50°C water-based drilling fluid is 9.5°C, the best cooling flow rate is about 0.52 m/s, and the average Reynolds number is 4966. In addition, the pressure difference between the two ends of the heat exchanger is 5.3 to 12.6 kPa, and the greater the flow rate, the greater the pressure difference.

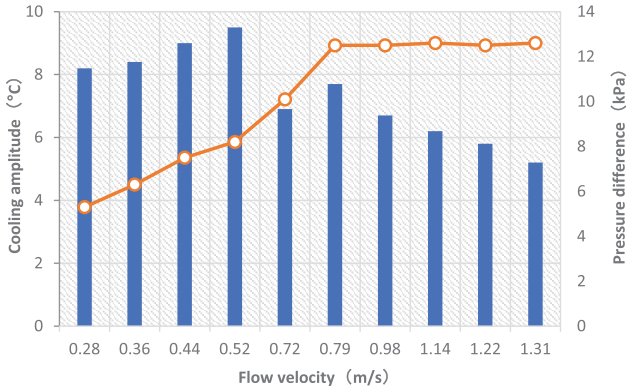

Figure 8: Comparison of cooling effect and pressure difference of heat exchanger at different flow rates of water-based drilling fluid

For water-based drilling fluids, the empirical correlation is derived:

$$Nu = 0.031 Re^{0.79} Pr^{0.36} \left(R^2 = 0.91\right)$$

where the higher exponent for Re reflects enhanced turbulence from bentonite particles.

3.2.2 Cooling Experiment Analysis under Different Temperature Conditions

As shown in Fig. 9 and 10, the higher the temperature of the water-based drilling fluid and the lower the temperature of the coolant, the larger the temperature difference across the heat exchanger, leading to enhanced heat transfer efficiency. The coolant at −10°C can reduce the water-based drilling fluid at 80°C, at a flow rate of 0.52 m/s, to 48°C (a decrease of 32°C). The higher the temperature of the water-based drilling fluid, the smaller the pressure difference between the two ends of the heat exchanger will be.

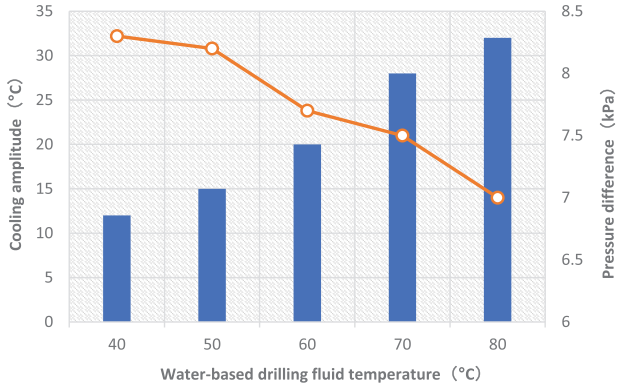

Figure 9: Comparison of cooling effect and heat exchanger pressure difference at different water-based drilling fluid temperatures

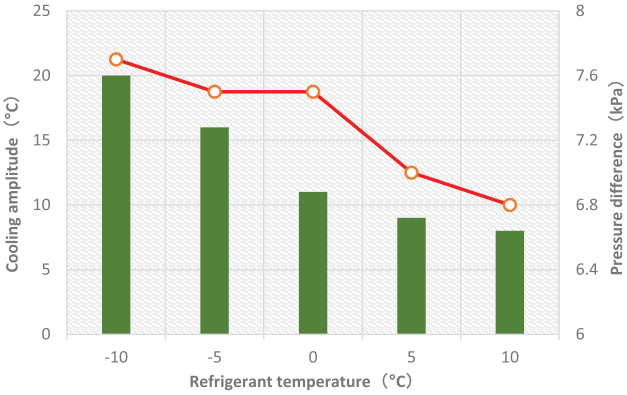

Figure 10: Comparison of cooling effect and heat exchanger pressure difference at different refrigerant temperatures

3.2.3 Cooling Experimental Analysis under Different Viscosity Conditions

As illustrated in Figs. 11 and 12, at low flow rates, the 10 mPa·s water-based drilling fluid exhibits a larger temperature drop (cooling range) compared to the 2 mPa·s fluid. As flow rate increases, both systems show a consistent expansion in their cooling ranges. This behavior arises from the interplay of two competing mechanisms: higher viscosity elevates boundary layer thermal resistance, which suppresses heat transfer and reduces the cooling range; conversely, a lower specific heat capacity enables more significant temperature reduction under identical heat exchange conditions.

Additionally, increased fluid viscosity directly corresponds to greater pressure differentials across the heat exchanger.

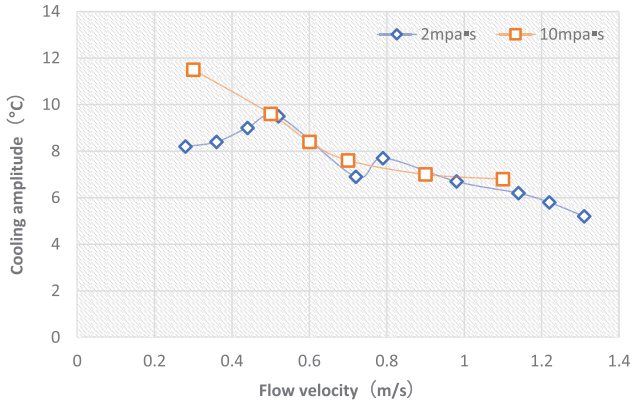

Figure 11: Comparison of cooling effect of water-based drilling fluid under different viscosity

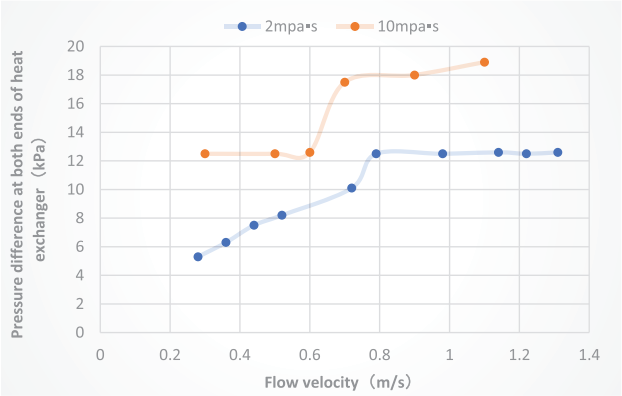

Figure 12: Comparison of heat exchanger pressure difference under different viscosity of water-based drilling fluid

According to the convective thermal resistance formula ($R_{convection} = 1/(hA)$), where h represents the convective heat transfer coefficient and A represents the heat transfer area), the increase in fluid viscosity directly leads to a decrease in h. This is because high-viscosity fluids exhibit greater flow resistance, accompanied by a decrease in molecular mobility, which in turn weakens the momentum and heat transfer efficiency at the fluid-heat exchanger interface, thereby increasing $R_{convection}$.

This viscosity-based change in thermal resistance is directly reflected in the cooling performance: under the same flow rate conditions, due to the presence of bentonite, the maximum cooling range of water-based drilling fluids with higher viscosity (32°C) is slightly lower than that of water-based drilling fluids with lower viscosity (34°C). This observation clearly indicates that the increase in fluid viscosity intensifies the obstacles to convective heat transfer, making the cooling efficiency more likely to be suppressed.

3.2.4 Cooling Experimental Analysis under Different Heat Exchanger Structure Conditions

As shown in Figs. 13 and 14, under the same hot fluid flow rate, the cooling rate of water-based drilling fluid after passing through the coil is significantly improved, increasing from 9.6°C to over 30°C. The pressure drop also increases, rising from 12.5 to 38 kPa. At a flow rate of 3–4 m/s in the ground manifold, the cooling rate of the coil heat exchanger remains above 20°C. The coil configuration demonstrates a significantly higher Nusselt number compared to the straight-pipe design, reflecting enhanced convective heat transfer performance due to secondary flow effects and increased residence time [26].

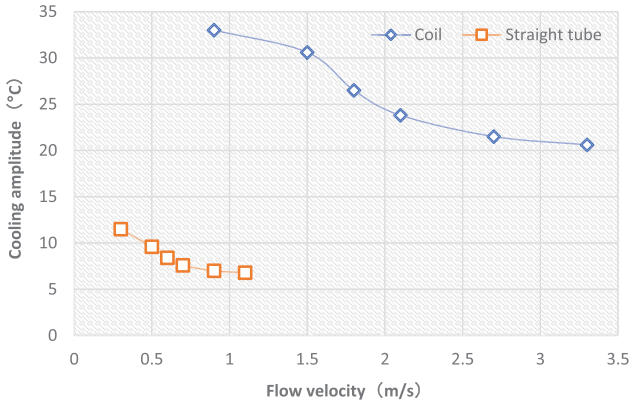

Figure 13: Comparison of cooling effects under different heat exchanger structures of water-based drilling fluid

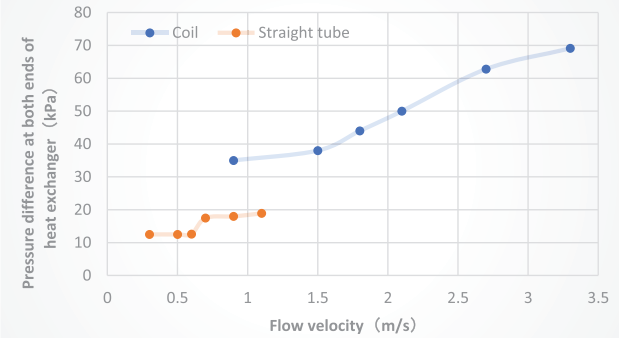

Figure 14: Comparison of pressure difference of heat exchanger under different heat exchanger structures of water-based drilling fluid

Heat exchanger structure affects cooling efficiency by altering area, flow perturbation, and pressure drop:

Enhanced effects of surface area and secondary flow: Coiled tube heat exchangers outperform straight tubes (water-based drilling fluid cooling range increases from 9.6°C to over 30°C) due to: Increased heat transfer area (≈5× greater for 10 m coil vs. 2 m straight tube in the document); Curvature-induced radial secondary flow disrupting the boundary layer, reducing convective resistance (higher Nusselt number Nu, which correlates positively with h).

Pressure drop as a trade-off: The coiled structure increases flow resistance (frictional + local resistance), significantly raising pressure drop (from 12.5 to 38 kPa for water-based fluids). For

high-viscosity oil-based fluids, coil pressure drop reaches 389 kPa at 2.5 m/s, driven by combined effects of viscosity-dependent friction factor (f) and velocity squared v^2 (Darcy-Weisbach equation: Delta$\Delta P = F \cdot L \rho v^2/2d$.

3.3 Experimental Analysis of Different Factors under Water-Based and Coil Conditions

3.3.1 Cooling Experiment Analysis under Different Flow Rate Conditions

As shown in Figs. 15 and 16, under the same hot fluid flow rate, the cooling rate of water-based drilling fluid after passing through the coil is significantly improved, from 9.6°C to over 30°C, and the pressure drop also increases, from 12.5 to 38 kPa. At a flow rate of 3–4 m/s in the ground manifold, the cooling rate of the coil heat exchanger remains above 20°C. The enhanced heat transfer in coiled tubes (ΔT increase of 30°C) is attributed to a 40% larger surface area and prolonged residence time ($\tau = 1.8$, 0.9 s in straight tubes).

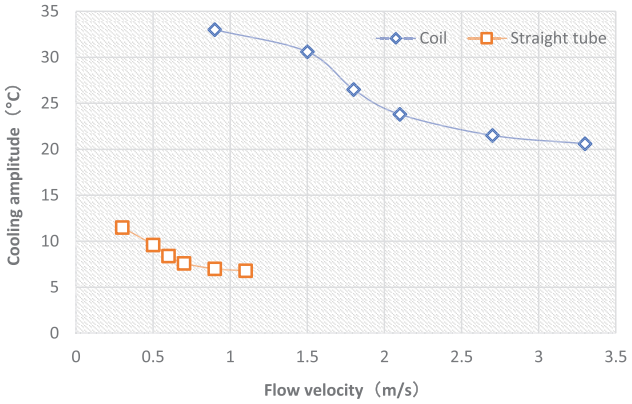

Figure 15: Comparison of cooling effects of water-based drilling fluid at different flow rates

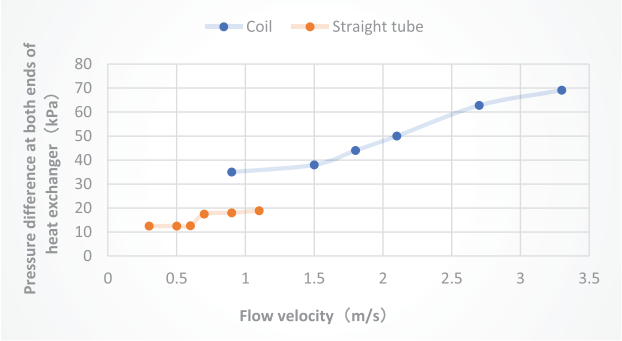

Figure 16: Comparison of pressure difference at different flow rates of water-based drilling fluid

3.3.2 Cooling Experiment Analysis under Different Temperature Conditions

As shown in Fig. 17, under different refrigerant temperatures, the cooling performance of water-based drilling fluid after passing through the coil at a flow rate of 1.5 m/s is effective, with the typical cooling rate reaching more than 20°C. In the −10°C refrigerant environment, it reached 41.3°C. If the temperature difference is further increased, it can be predicted that the drilling fluid temperature can be reduced from 80°C to between 30°C and 40°C.

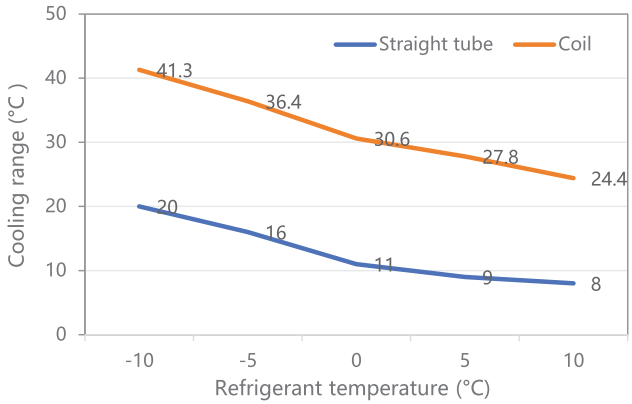

Figure 17: Comparison of cooling effects of water-based drilling fluid coil at different coolant temperatures

3.4 Experimental Analysis of Different Factors under Oil-Based and Coil Conditions

3.4.1 Cooling Experiment Analysis under Different Flow Rate Conditions

As shown in Fig. 18, the cooling rate of oil-based drilling fluid at low flow rates is not much different from that of water-based drilling fluid. When the flow rate reaches 1.5 m/s, the cooling rate is significantly greater than that of water-based drilling fluid. This is attributed to the lower specific heat capacity of oil-based drilling fluids, which results in a more significant temperature drop under identical heat exchange conditions. At the flow rate of 2.5 m/s, the cooling rate of oil-based drilling fluid is still above 30°C.

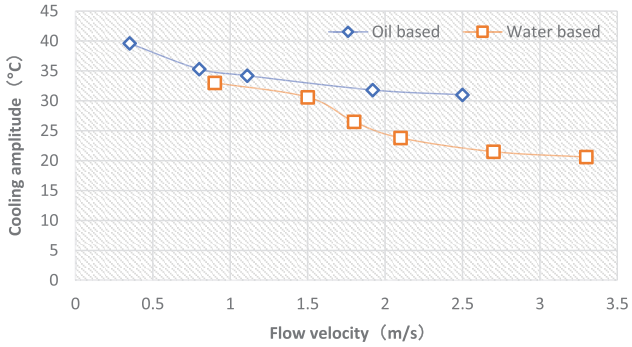

Figure 18: Comparison of cooling effect of oil-based drilling fluid coil and different flow rates

As shown in Fig. 19, the viscosity of the oil-based drilling fluid is 120 mPa·s, so the pressure difference across the coil heat exchanger has increased significantly. At a flow rate of 2.5 m/s, the pressure difference across the coil reaches 389 kPa.

3.4.2 Cooling Experiment Analysis under Different Temperature Conditions

As shown in Figs. 20 and 21, in an environment with a coolant temperature of 0°C, the maximum cooling range of oil-based drilling fluid passing through the coil at a flow rate of 1.11 m/s is 36.7°C. After the temperature of the drilling fluid reaches 70°C, the cooling range no longer increases. Further

reducing the temperature of the coolant to −10°C can cool the oil-based drilling fluid from 60°C to 15.5°C, resulting in a cooling range of 44.5°C.

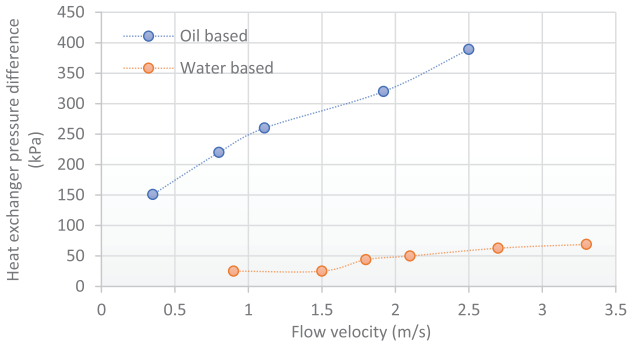

Figure 19: Comparison of pressure difference between oil-based drilling fluid coil and heat exchanger at different flow rates

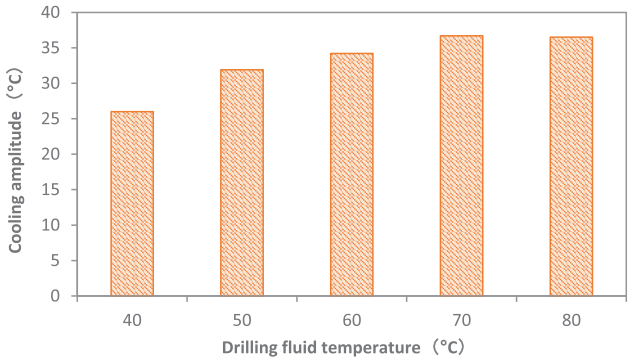

Figure 20: Comparison of cooling effects of oil-based drilling fluid coil and different drilling fluid temperatures

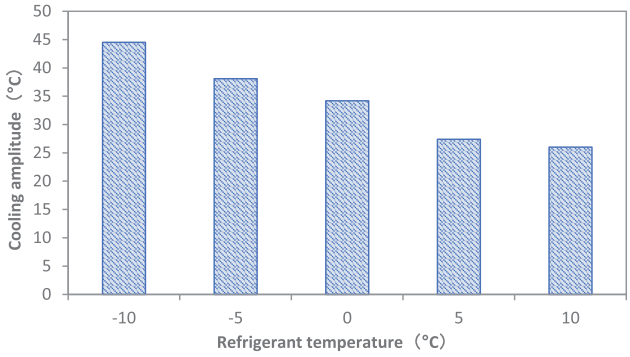

Figure 21: Comparison of cooling effects of oil-based drilling fluid coil at different coolant temperatures

4 Conclusion

This study constructed an experimental model of a drilling fluid ground cooling system to systematically investigate the effects of flow velocity, temperature difference, heat exchanger structure, and fluid medium on the cooling efficiency of drilling fluids in ultra-deep wells. For the first time, it quantified the law of multi-factor coupling effects within a unified experimental framework, filling the gap in existing research regarding the analysis of cooling mechanisms under complex working conditions.

Key findings include: At a medium flow velocity (0.32 m/s, Re ≈ 4900), the turbulent flow effect and contact time reach an optimal balance, achieving the maximum cooling range (34°C), which provides critical flow regime parameters for heat exchanger size design. The coil structure, through secondary flow enhancement and increased heat transfer area, improves cooling efficiency by more than 300% compared to straight tubes (cooling range exceeding 30°C). Although accompanied by increased pressure drop (up to 38 kPa), it offers a structural optimization direction for high-efficiency cooling solutions. Despite bentonite particles in water-based drilling fluids increasing convective thermal resistance due to higher viscosity (resulting in a slightly lower cooling range than pure water), they still achieve a 32°C temperature reduction at the optimal flow velocity (0.52 m/s), verifying the feasibility of cooling high-solid-phase fluids.

These results provide clear guidance for field applications: Ultra-deep well drilling should prioritize coil heat exchangers, matched with a medium flow velocity of 0.3–0.5 m/s to balance efficiency and energy consumption. For high-viscosity drilling fluids, thermal resistance should be reduced through flow regime optimization (e.g., turbulence-promoting structures) rather than simply increasing flow velocity. This research not only provides quantitative basis for the engineering design of drilling fluid cooling systems but also establishes a coupling analysis method of "flow regime-thermal resistance-structure," laying a theoretical foundation for high-temperature control technologies in deep energy development.

Acknowledgement: Not applicable.

Funding Statement: This research work was supported by the project is supported by the National Science and Technology Major Project (No. 2025ZD1401900, No. 2025ZD1401905), the Key Core Technology Research Project of China National Petroleum Corporation (2024ZG26), the Youth Science and Technology Program of China National Petroleum Corporation (2024DQ03086), the Joint Foundation Program of National Natural Science Foundation of China (U24B2030), the China National Petroleum Corporation (CNPC) Project (2023DQ03-01), and the CNPC Research Institute of Engineering Technology Co., Ltd. Project (CPET202320).

Author Contributions: The authors confirm contribution to the paper as follows: study conception and design: Jiangshuai Wang, Zixiao Song, Yufei Chen, Song Deng; data collection: Bohan Zheng, Ke Xu; analysis and interpretation of results: Qianyu Ren; draft manuscript preparation: Bei Wang. All authors reviewed the results and approved the final version of the manuscript.

Availability of Data and Materials: The datasets generated and/or analyzed during the current study are available from the corresponding author on reasonable request.

Ethics Approval: Not applicable.

Conflicts of Interest: The authors declare no conflicts of interest to report regarding the present study.

References

1. Wang Z. Current situation and development suggestions for drilling fluid technologies in China. Petrol Drill Tech. 2023;51(4):114–23. doi:10.11911/syztjs.2023028.
2. Ali M, Jarni HH, Aftab A, Ismail AR, Saady NMC, Sahito MF, et al. Nanomaterial-based drilling fluids for exploitation of unconventional reservoirs: a review. Energies. 2020;13(13):3417. doi:10.3390/en13133417.
3. Luo YX, Wang WJ, Jin JB. Key drilling fluid technology in the ultra deep section of Well Ying-1 in the Shun-bei Oil and Gas Field. Pet Drill Tech. 2019;47(03):113–20.
4. Gautam S, Guria C, Rajak VK. A state of the art review on the performance of high-pressure and high-temperature drilling fluids: towards understanding the structure-property relationship of drilling fluid additives. J Petrol Sci Eng. 2022;213:110318. doi:10.1016/j.petrol.2022.110318.
5. Weintritt DJ, Hughes RG. Factors involved in high-temperature drilling fluids. J Petrol Technol. 1965;17(6):707–16. doi:10.2118/1043-pa.
6. Basfar S, Ahmed A, Elkatatny S. Stability enhancing of water-based drilling fluid at high pressure high temperature. Arab J Sci Eng. 2021;46(7):6895–901. doi:10.1007/s13369-020-05126-w.
7. Mohamed A, Salehi S, Ahmed R. Significance and complications of drilling fluid rheology in geothermal drilling: a review. Geothermics. 2021;93:102066. doi:10.1016/j.geothermics.2021.102066.
8. Liu N, Zhang D, Gao H, Hu Y, Duan L. Real-time measurement of drilling fluid rheological properties: a review. Sensors. 2021;21(11):3592. doi:10.3390/s21113592.
9. Liu J, Zhang T, Sun Y, Lin D, Feng X, Wang F. Insights into the high temperature-induced failure mechanism of bentonite in drilling fluid. Chem Eng J. 2022;445:136680. doi:10.1016/j.cej.2022.136680.
10. Zhang Z, Wei Y, Xiong Y, Peng G, Wang G, Lu J, et al. Influence of the location of drilling fluid loss on well-bore temperature distribution during drilling. Energy. 2022;244:123031. doi:10.1016/j.energy.2021.123031.
11. Kozhevnykov AO, Dreus AY, Liu B, Sudakov AK. Drilling fluid circulation rate influence on the contact temperature during borehole drilling. Sci Bull Natl Min Univ. 2018;1:35–42. doi:10.29202/nvngu/2018-1/14.
12. Zhang Z, Xiong Y, Pu H, Sun Z. Effect of the variations of thermophysical properties of drilling fluids with temperature on wellbore temperature calculation during drilling. Energy. 2021;214:119055. doi:10.1016/j.energy.2020.119055.
13. Allawi RH, Najem MA, Sagger MA, Abd SM. Effect of temperature on drilling mud. J Phys Conf Ser. 2019;1279(1):012054. doi:10.1088/1742-6596/1279/1/012054.
14. Zakaria MF, Husein M, Hareland G. Novel nanoparticle-based drilling fluid with improved characteristics. In: SPE International Oilfield Nanotechnology Conference and Exhibition; 2012 Jun 12–14; Noordwijk, The Netherlands. doi:10.2118/156992-ms.
15. Shaymanova RS, Urazov MK, Yuldosheva DN. Improvement of drilling fluid for con-struction of wells. Multidiscip J Sci Technol. 2022;2(2):12–4.
16. Vryzas Z, Kelessidis VC. Nano-based drilling fluids: a review. Energies. 2017;10(4):540. doi:10.3390/en10040540.
17. Li J, Yang P, Guan J, Sun Y, Kuang X, Chen S. A new type of whole oil-based drilling fluid. Petrol Explor Dev. 2014;41(4):538–44. doi:10.1016/s1876-3804(14)60064-1.
18. Zhu W, Zheng X. Effective modified xanthan gum fluid loss agent for high-temperature water-based drilling fluid and the filtration control mechanism. ACS Omega. 2021;6(37):23788–801. doi:10.1021/ac-somega.1c02617.
19. Wang X, Wu P, Chen Y, Zhang E, Ye X, Huang Q, et al. Research on nanoparticle-enhanced cooling technology for oil-based drilling fluids. Appl Sci. 2024;14(23):10969. doi:10.3390/app142310969.
20. Arghand T, Javed S, Trüschel A, Dalenbäck JO. Control methods for a direct-ground cooling system: an experimental study on office cooling with ground-coupled ceiling cooling panels. Energy Build. 2019;197:47–56. doi:10.1016/j.enbuild.2019.05.049.

21. Ren J, Liu J, Zhou S, Kim MK, Song S. Experimental study on control strategies of radiant floor cooling system with direct-ground cooling source and displacement ventilation system: a case study in an office building. Energy. 2022;239:122410. doi:10.1016/j.energy.2021.122410.
22. Arghand T, Javed S, Dalenbäck JO. Combining direct ground cooling with ground-source heat pumps and district heating: borehole sizing and land area requirements. Geothermics. 2022;106:102565. doi:10.1016/j.geothermics.2022.102565.
23. Arghand T, Javed S, Trüschel A, Dalenbäck JO. Influence of system operation on the design and performance of a direct ground-coupled cooling system. Energy Build. 2021;234:110709. doi:10.1016/j.enbuild.2020.110709.
24. Wagner AM, Maakestad JB, Yarmak E Jr, Douglas TA. Off-grid solar powered ground cooling system. J Cold Reg Eng. 2024;38:06023002. doi:10.1061/jcrgei.creng-605.
25. Bernardin C, Olla S. Fourier's law for a microscopic model of heat conduction. J Stat Phys. 2005;121(3):271–89. doi:10.1007/s10955-005-7578-9.
26. Deng G, Cui X, Wang X. Comparison of heat transfer performance between helical groove pipe and straight pipe. Refrig Air Cond. 2012;26(2):209–12. (In Chinese).